arXiv:1512.05226v1 [nlin.PS] 15 Dec 2015

On the dynamics of solitary wave solutions supported by the model of mutually penetrating continua

Sergii Skurativskyi [1] **, Vjacheslav Danylenko**

Subbotin Institute of Geophysics, NAS of Ukraine, Bohdan Khmelnytskyi str. 63-G, Kyiv, UKRAINE

Abstract: The model we deal with is the mathematical model for mutually penetrating continua one of which is the carrying medium obeying the wave equation whereas the other one is the oscillating inclusion described by the equation for oscillators. These equations of motion are closed by the cubic constitutive equation for the carrying medium. Studying the wave solutions we reduce this model to a plane dynamical system of Hamiltonian type. This allows us to derive the relation describing the homoclinic trajectory going through the origin and obtain the solitary wave with infinite support. Moreover, there exist a limiting solitary wave with finite support, i.e. compacton. To model the solitary waves dynamics, we construct the three level finite-difference numerical scheme and study its stability. We are interested in the interaction of the pair of solitary waves. It turns out that the collisions of solitary waves have non-elastic character but the shapes of waves after collisions are preserved.

Keywords: travelling wave solutions; homoclinic curve; solitary waves; collision of solitons

1 Introduction

Natural geomaterials are highly heterogeneous and interact intensively with the environment. In these conditions the peculiarities of internal medium's structure, namely discreteness and oscillating dynamics [1, 6], can manifest. To incorporate these features of media, the mathematical model for mutually penetrating continua is used [5, 9]. This model consists of the wave equation for carrying medium and equations of motion for oscillating continuum which is regarded as the set of partial oscillators. To generalize the linear counterpart of this model [5, 9], the nonlinearity has been incorporated in the equation of state for carring medium [2, 3, 7] and in the kinetics for oscillator's equations of motion. We thus are going to treat the following mathematical model

$$\rho\frac{\partial^2 u}{\partial t^2}=\frac{\partial \sigma}{\partial x}-m\rho\frac{\partial^2 w}{\partial t^2},\qquad \frac{\partial^2 w}{\partial t^2}+\Phi\left(w-u\right)=0, \tag{1}$$

where ρ is medium's density, u and w are the displacements of carrying medium and oscillator from the rest state, $m\rho$ is the density of oscillating continuum. To close model (1), we apply the cubic constitutive equation for the carrying medium $\sigma = e_1u_x + e_3u_x^3$ and $\Phi(x) = \omega^2x + \delta x^3$. The novelty of this model lies in the taking into account the cubic terms in the expressions for σ and Φ.

In this report we consider the properties of wave solutions having the following form

$$u=U(s), w=W(s), s=x-Dt, \tag{2}$$

where the parameter D is a constant velocity of the wave front. Inserting (2) into model (1), it easy to see that the functions U and W satisfy the dynamical system

$$D^2U'=\rho^{-1}\sigma\left(U'\right)-mD^2W',\quad W''+\Omega^2\left(W-U\right)+\delta D^{-1}\left(W-U\right)^3=0,$$

[1] Corresponding author: skurserg@gmail.com

where $\Omega = \omega D^{-1}$.

This system can be written in the form

$$W' = \alpha_1 R + \alpha_3 R^3,\ U' = R,\ (\alpha_1 + 3\alpha_3 R^2)R' + \Omega^2(W-U) + \delta D^{-2}(W-U)^3 = 0, \quad (3)$$

where $\alpha_1 = \dfrac{e_1 - D^2\rho}{m\rho D^2}$, $\alpha_3 = \dfrac{e_3}{m\rho D^2}$. Through the report we fix $e_1 = 1$, $e_3 = 0.5$, $m = 0.6$, $\omega = 0.9$ in numerical treatments.

1.1 Solitary waves in the model with the linear equation of motion for oscillating inclusions

At first, consider system (3) at $\delta = 0$. Excluding the variable W, system (3) is reduced to the planar system

$$\begin{aligned} \left(\alpha_1 + 3\alpha_3 R^2\right)^2 R' &= Z\left(\alpha_1 + 3\alpha_3 R^2\right)^2, \\ \left(\alpha_1 + 3\alpha_3 R^2\right)^2 Z' &= -\left[6\alpha_3 R Z^2 + \Omega^2\left(\left(\alpha_1 - 1\right)R + \alpha_3 R^3\right)\right]\left(\alpha_1 + 3\alpha_3 R^2\right), \end{aligned} \quad (4)$$

which admits the Hamiltonian

$$H = \frac{1}{2}Z^2\left(\alpha_1 + 3\alpha_3 R^2\right)^2 + \frac{\Omega^2}{2}\left[\alpha_3^2 R^6 + \frac{4\alpha_1 - 3}{2}\alpha_3 R^4 + \left(\alpha_1^2 - \alpha_1\right)R^2\right] = \text{ const.}$$

Since solitary waves correspond to homoclinic loops, we thus need to state the conditions when saddle separatrices form a loop. Omitting the detail description [8] of phase plane of dynamical system (4), let us consider the fixed saddle points and their separatrices only. System (4) has the fixed points $O(0;0)$ and $A_\pm = \pm\sqrt{(1-\alpha_1)/\alpha_3}$ if $(1-\alpha_1)/\alpha_3 > 0$. It easy to see that the origin is a center at $\alpha_1 < 0$, whereas it is a saddle if $0 < \alpha_1 < 1$.

Therefore, we can restrict ourself by the case when $0 < \alpha_1 < 1$ only. So, the homoclinic trajectories that go through the origin satisfy the equation $H = 0$. From this it follows the relation for $Z = Z(R)$ and the expression $s - s_0 = \int dR/Z(R)$ for homoclinic loop which can be written in the explicit form

$$\begin{aligned} s - s_0 = \frac{3}{2\Omega}\arcsin\left(\frac{4\alpha_3 r - 3 + 4\alpha_1}{\sqrt{9 - 8\alpha_1}}\right) - \frac{1}{2\Omega}\sqrt{\frac{\alpha_1}{1-\alpha_1}}\times \\ \ln\left(\frac{1}{r} + \frac{3\alpha_3 - 4\alpha_1\alpha_3}{4\left(\alpha_1 - \alpha_1^2\right)} + \sqrt{\left\{\frac{1}{r} + \frac{3\alpha_3 - 4\alpha_1\alpha_3}{4\left(\alpha_1 - \alpha_1^2\right)}\right\}^2 - \frac{\alpha_3^2\left(9 - 8\alpha_1\right)}{16\left(\alpha_1 - \alpha_1^2\right)^2}}\right)\Bigg|_{r_0}^{r}, \end{aligned} \quad (5)$$

where $r = R^2$. The typical phase portrait of dynamical system (4) is depicted in fig. 1a. The pair of homoclinic orbits are drawn with the bold curves. Solution (5) corresponds to the soliton solution with infinite support at $0 < \alpha_1 < 1$.

When α_1 tends to zero, the angles between separatrices of saddle point O are growing. As a result, at $\alpha_1 = 0$ we obtain the degenerate phase portrait presented in fig.1b. The bold lines mark the orbits corresponding to solitary wave solutions with finite support (compacton). These orbits are described by the following expressions

$$R = U_s' = \begin{cases} \sqrt{\frac{3}{2\alpha_3}}\sin\left(\frac{\Omega s}{3}\right), \frac{\Omega s}{3} \in [0;\pi] \\ 0, \frac{\Omega s}{3} \notin [0;\pi]. \end{cases}$$

This regime can be thought as a limit state for solution (5) with infinite support.

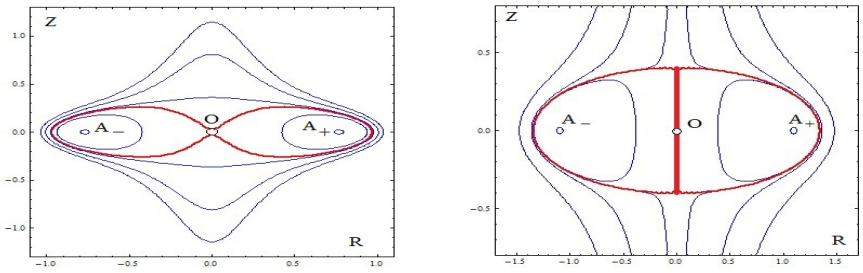

a b

Figure 1: The phase portraits for system (4) at a: $\alpha_1 < 1$ ($D = 0.9$) and b: $\alpha_1 = 0$ ($D = 1$).

1.2 Homoclinic loops in the model with cubic nonlinearity in the equation of motion for oscillating inclusions

If $\delta \neq 0$, then system (3) does not reduce to the dynamical system in the plane $(R; R')$. But the first integral for (3) can still be derived in the form

$$I = \Omega^2 (W-U)^2 + \frac{\delta}{2D^2}(W-U)^4 + \alpha_3^2 R^6 + \frac{4\alpha_1 - 3}{2}\alpha_3 R^4 + \left(\alpha_1^2 - \alpha_1\right) R^2.$$

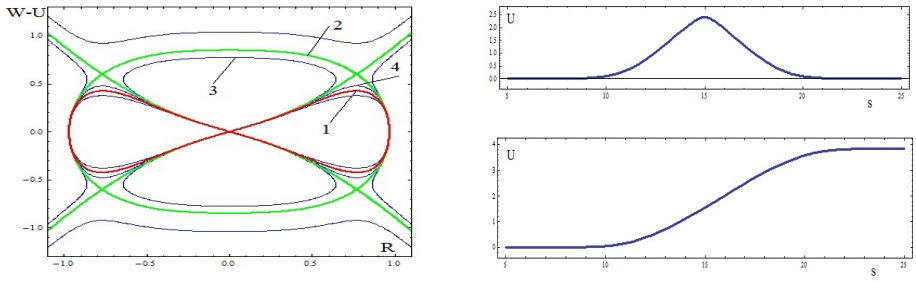

Figure 2: Left: Position of level curves $I(\delta) = 0$ at different values of δ. Curve 1 is plotted at $\delta = 0$, curve 2 at δ_0, curve 3 at $\delta = -1.5 > \delta_0$, curve 4 at $\delta = -2.7 < \delta_0$. Right: Homoclinic trajectories from the left diagram corresponding to $\delta = -2.7 < \delta_0$ (upper panel) and $\delta = -1.5 > \delta_0$ (lower panel).

Consider the position and the form of homoclinic trajectories when the parameter δ is varied. Since homoclinic loops are described by the level curve $I = 0$, we plot the set of curve $I(\delta) = 0$ (fig.2). Starting from the loop $I(0) = 0$ which coincides with the orbits of fig.1a, we see that increasing δ causes the attenuation of loop's size along vertical exis. If δ decreases, loop's size grows, but at δ_0 the additional heterocycle connecting four new saddle points appears. The bifurcational value δ_0 can be derived via analysing the function $I(\delta)$. Namely, solving the biquadratic equation $I = 0$ with respect to $W - U$, several branches of level curves are obtained. The condition of contact for two branches leads us to a qubic equation with respect to R^2 with zero discriminant. Then $\delta_0 = -\frac{\alpha_3 \Omega^4 D^2}{(\alpha_1 - 1)^2}$ or $\delta_0 = \frac{27\alpha_3\Omega^4 D^2}{\alpha_1^2(9-8\alpha_1)}$.

So, if $D = 0.9$, then $\delta_0 = -2.24732$. From the figure 2 it follows that for $\delta < \delta_0$ the homoclinic loops are placed in the vertical quarters of the phase plane. Note that the profiles of the resulting solitary waves are different (fig.2(right panel)), namely, at $\delta < \delta_0$ the U profile looks like a bell-shape curve, whereas at $\delta > \delta_0$ it is a kink-like regime.

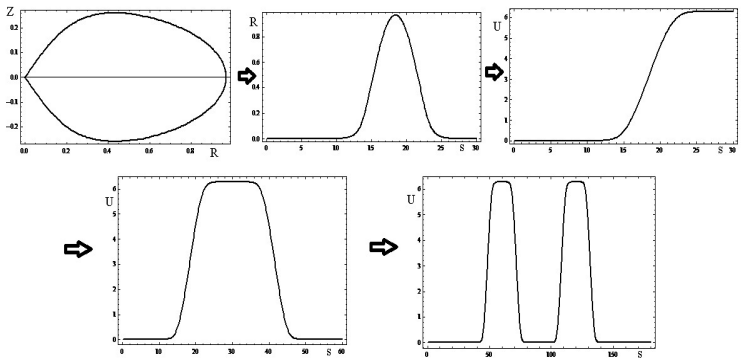

Figure 3: The construction of initial data for numerical scheme.

1.3 The numerical scheme for the model (1)

To model the soliton dynamics, we construct the three level finite-difference numerical scheme for model (1) and study its stability.

Let us construct the numerical scheme for model (1) in the region $\Sigma = [0 \le x \le L] \times [0 \le t \le T]$ with grid lines $x = ih$ and $t = j\tau$, where h, τ are constant, $i = 1...N$. Consider three level numerical scheme. Denote $u = u(t_{j+1})$, $v = u(t_j)$, $q = u(t_{j-1})$, and $K = w(t_{j+1})$, $G = w(t_j)$, $F = w(t_{j-1})$. We use the following difference approximation of derivatives

$$\frac{\partial^2 u}{\partial t^2} \approx \frac{u_i - 2v_i + q_i}{\tau^2}, \quad \frac{\partial^2 u}{\partial x^2} \approx r\frac{u_{i-1} - 2u_i + u_{i+1}}{h^2} + (1-r)\frac{v_{i-1} - 2v_i + v_{i+1}}{h^2},$$

$$\frac{\partial u}{\partial x} \approx \frac{v_{i+1} - v_{i-1}}{2h}, \quad \frac{\partial^2 w}{\partial t^2} \approx \frac{K_i - 2G_i + F_i}{\tau^2}, \quad w - u \approx \frac{3G_i - F_i}{2} - \frac{3v_i - q_i}{2} \equiv \psi_i.$$

Thus, if $r \neq 0$, then we obtain the three level implicit scheme:

$$A_i u_{i-1} + C_i u_i + B_i u_{i+1} = Y_i, \quad K_i = 2G_i - F_i - \tau^2\omega^2\psi_i - \tau^2\delta\psi_i^3, \tag{6}$$

where $A_i = B_i = \dfrac{r}{h^2}\varphi$, $C_i = -2\dfrac{r}{h^2}\varphi - \dfrac{1}{\tau^2}$, $\varphi = \rho^{-1}\left(e_1 + 3e_3\left(\dfrac{v_{i+1} - v_{i-1}}{2h}\right)^2\right)$,

$$Y_i = -\left(\varphi\frac{v_{i-1} - 2v_i + v_{i+1}}{h^2}(1-r) + m\omega^2\psi_i + m\delta\psi_i^3 + \frac{2v_i - q_i}{\tau^2}\right).$$

System of algebraic equations (6) can be solved by the sweep method. The necessary conditions of the sweep method stability ($|A_i| + |B_i| \le |C_i|$) are fulfilled. To get the restrictions for spatial and temporal steps, the Fourier stability method, being applied to linearized scheme (6), is used. Let us fix the values of the parameters $e_1 = 1$, $e_3 = 0.5$, $\rho = 1$, $\omega = 0.9$, $m = 0.6$, $D = 0.9$, and the parameters of the numerical scheme $L = 30$, $N = 200$, $r = 0.3$, $h = L/N$, $\tau = 0.05$.

Let us construct the initial data v_i, q_i, G_i, F_i for numerical simulation on the base of solitary waves. To do this, we integrate dynamical system (4) with initial data $R(0) = 10^{-8}$, $Z(0) = 0$, $s \in [0; L]$ and choose the right homoclinic loop in the phase portrait (fig.1). Then the profiles of $W(s)$, $U(s)$, and $R(s)$ can be derived. Joining the proper arrays, we can build the profile in the form of arch:

$$v = U(ih) \cup U(L - ih),\ q = u(x + \tau D) = [U(ih) + \tau DR(ih)] \cup [U(L - ih) + \tau DR(L - ih)]\,.$$

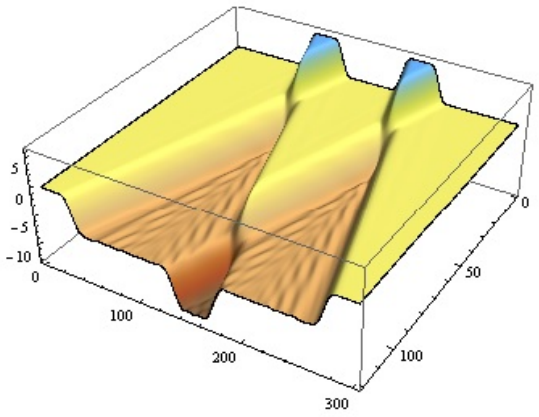

Figure 4: The propagation of solitary waves at $\delta = 0$ starting from the initial profile depicted in the figure 3.

The arrays G and F are formed in similar manner. Combining two arches and continuing the steady solutions at the ends of graph, we get more complicated profile.The sequence of steps for profile construction is depicted in figure 3 in detail. We apply the fixed boundary conditions, i.e. $u(x = 0, t) = v_1$, $u(x = Kh, t) = v_K$, where K is the length of an array.

Starting from the two-arch initial data, we see (fig.4) that solitary waves move to each other, vanish during approaching, and appear with negative amplitude and shift of phases. After collision in the zones between waves some ripples are revealed. Secondary collision of waves are watched also. Note that the simulation of compacton solutions displays similar properties.

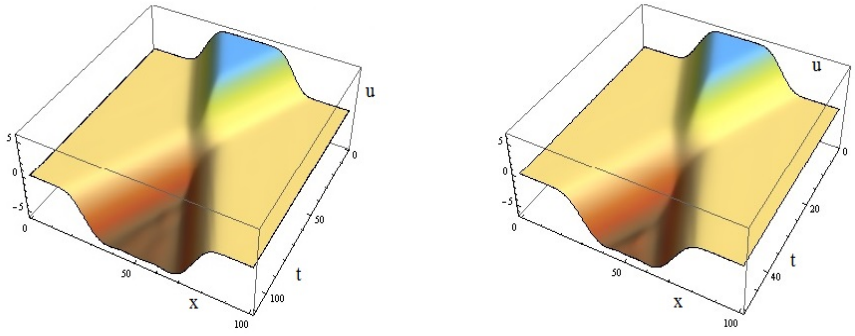

Figure 5: Solitary waves dynamics at $\delta = -0.2$ and $\delta = 1.3$.

Propagation of solitary waves at $\delta \neq 0$ depends on the sign of δ. Analysing the diagrams of figures 5, we see that for $\delta > 0$ the collision of waves is similar to the collision at $\delta = 0$. Behaviour of waves after interaction does not change essentially when $\delta < 0$ and close to zero. But at $\delta = -0.3$ after collision the amplitude of solution is increasing in the place of soliton's intersection (fig.6) and after a while the solution is destroyed.

This suggests that we encounter the unstable interaction of solitary waves or the numerical scheme we used possesses spurious solutions. But if we take half spatial step and increase the scheme parameter r up to 0.8, the scenario of solitary waves collision is not

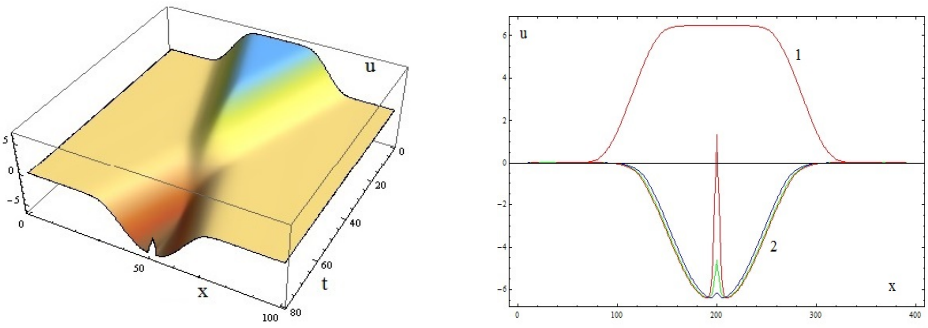

Figure 6: Solitary waves dynamics at $\delta = -0.3$. In the right panel the curve 1 is the initial profile, whereas other curves 2 are the forms of solutions just before blowup.

changed qualitatively. Therefore, the assertion on the unstable nature of collision is more preferable.

2 Conclusions

So, in this report, we have presented the novel nonlinear generalization of model for media with oscillating inclusions. It is important for application that the new parameters e_3 and δ have clear physical meaning. As it was shown in subsections 1.1 and 1.2, this model possesses the solitary waves of different types including compactons. We have considered the conditions of their existence and bifurcations when the parameters of nonlinearity were varied. The exact solutions describing the solitary waves with both unbounded and compact support were derived. Analysing the expression (5) and Fig. 2a, we should emphasize that the characteristics of solitary waves crucially depend on the dynamics of oscillating inclusions. To study the properties of solitary waves and their interactions, we have proposed the effective numerical scheme based on the finite difference approximation of the continious model. In particular, we have found out the conditions when the stable propagation of solitons and their collisions are observed. It turned out that the nonlinearity of the oscillating dynamics describing by Φ affects not only the form of solitary waves but their stability properties in collisions (Fig. 6). Finally, there are solitary waves moving without preserving of their selfsimilar shapes. While the numerical results concerning the stable properties of single solitary wave can be confirmed by analytical treatments [10], the studies of wave collisions require mostly the application of improved numerical schemes. The results presented above can be useful for modelling the behaviour of complex media in vibrational fields, for instance when we deal with the intensification of extracting oil and natural gas [4].

References

[1] Danylenko, V., Danevych, T., Makarenko, O., Skurativskyi, S., and Vladimirov, V. *Self-organization in nonlocal non-equilibrium media.* Subbotin int of geophysics NAS of Ukraine, Kyiv, 2011.

[2] Danylenko, V., and Skurativskyi, S. Resonance regimes of the spreading of nonlinear wave fields in media with oscillating inclusions. *Reports of NAS of Ukraine*, 11 (2008), 108–112.

[3] Danylenko, V., and Skurativskyi, S. Travelling wave solutions of nonlocal models for media with oscillating inclusions. *Nonlinear Dynamics and Systems Theory 4*, 12 (2012), 365–374.

[4] Nikolaevskiy, V. N. Mechanism and dominant frequencies of vibrational enhancement of yield of oil pools. *USSR Acad. Sci., Earth Science Sections*, 307 (1989), 570–575.

[5] Palmov, V. A. On a model of medium of complex structure. *Journal of Applied Mathematics and Mechanics*, 4 (1969), 768–773.

[6] Sadovskyi, M. A. Self-similarity of geodynamical processes. *Herald of the RAS*, 8 (1986), 3–12.

[7] Skurativskyi, S. Chaotic wave solutions in a nonlocal model for media with vibrating inclusions. *Journal of Mathematical Sciences*, 198(1) (2014), 54–61.

[8] Skuratovskii, S., and Skuratovskaya, I. Localized autowave solutions of the nonlinear model of complex medium. *Electronic Journal Technical Acoustics*, 6 (2010), http: ejta.org.

[9] Slepjan, L. I. Wave of deformation in a rod with flexible mounted masses. *Mechanics of Solids*, 5 (1967), 34–40.

[10] Vladimirov, V., Maczka, C., Sergyeyev, A., and Skurativskyi, S. Stability and dynamical features of solitary wave solutions for a hydrodynamic type system taking into account nonlocal effects. *Commun. in Nonlinear Science and Num. Simul.*, 19(6) (2014), 1770–1782.